CONSISTENT ALONG TRACK SHARPNESS IN A PUSH-BROOM IMAGING SYSTEM

Dennis D. Langer[1,2]*, Tor A. Johansen*[1,3]*, Asgeir J. Sørensen*[1,2]

[1] Norwegian University of Science and Technology (NTNU)
[2] Department of Marine Technology (IMT)
[3] Department of Engineering Cybernetics (ITK)

ABSTRACT

The along track spatial resolution in push broom imaging systems depends on platform parameters and imaging settings. This paper present a method for achieving a consistent spatial resolution for varying exposure times. We consider the geometry of a simplified push broom imaging system to derive relationships between spatial resolution, platform parameters (altitude, speed, focal length, slit width) and recording settings (exposure time, frame rate). The method is tested and verified using data from the HYPerspectral Smallsat for Ocean observation-1 (HYPSO-1). The spatial resolution is consistent over the exposure time range of 4.41ms to 49.3ms for low off-nadir angles when choosing frame rates according to the method.

***Index Terms*—** Push-broom imaging, mission planning, spatial resolution, along track field of view.

1. INTRODUCTION

A common intuition is that a decrease in Ground Sample Distance (GSD) leads to an increase in resolution. In other words, imaging a scene with more sample points per area improves spatial resolution. However, during the operation of and data processing from the HYPerspectral Smallsat for Ocean observation-1 (HYPSO-1) satellite, [1, 2], it was noticed in two cases that there is a limit to how dense a push broom imaging system can sample to improve the spatial resolution. In the first case, images with varying exposure times at the same frame rate had varying image sharpness. In the second case, a slew maneuver implemented to decrease GSD does not increase spatial resolution.

The main scientific contribution of this paper is 1) to illustrate how the along track field of view of a push broom imaging system and varying exposure time (which can be set independent from frame rate) influence along track spatial resolution, and 2) how a method for choosing the parameters to achieve a desired spatial resolution performs using the HYPSO-1 satellite.

This work was supported by the Research Council of Norway through the Centre of Excellence funding scheme NTNU AMOS (grant no. 223254), HYPSCI (grant no. 325961), NO Grants 2014 - 2021 under Project ELO-Hyp (contract no. 24/2020), the Norwegian Space Agency and the European Space Agency through PRODEX (no. 4000132515).

Section 2 reviews related work and defines terms. Section 3 shows an analysis of a simplified model of the along track sampling geometry of push-broom imaging systems to establish relationships between the base parameters listed in Table 1 and spatial resolution. Section 3 also presents a method of determining acquisition parameters to achieve a consistent image sharpness across varying exposure times and a simple method to estimate image sharpness. Section 4 presents the results of the analysis of data from HYPSO-1 with regards to spatial resolution. Section 5 provides concluding remarks.

2. BACKGROUND

Previous work related to planning operations with a push broom type imaging system discusses in detail the choice of parameters to achieve a desired GSD as a proxy for spatial resolution [3, 4, 5]. GSD is not a direct and complete indicator for spatial resolution [6, 7], especially when considering the along track field of view of a push-broom imaging system.

Spatial resolution is understood as the minimum distance between spatial features in the scene such that they can be distinguished in an image. This is also called the Ground Resolution Distance (GRD) [6]. The spatial resolution of an image can be determined by computing the Full Width Half Maximum (FWHM) of the Edge Spread Function (ESF), which is a relative spatial resolution metric in image space that quantifies image sharpness. The method used in Section 4 to determine the FWHM of the ESF of HYPSO-1 data follows a simplified manual procedure as shown in [8]. The GRD can be estimated by multiplying the FWHM of the ESF with the GSD [6]. The term image *sharpness* is used to refer to FWHM of the ESF and blurriness is the understood as the reciprocal of sharpness.

Launched in January 2022, the HYPSO-1 satellite is regularly delivering data from various targets around the earth with its push broom hyperspectral camera [1, 2]. HYPSO-1 is an experimental satellite with high configurability of recording settings and off-nadir pointing control.

3. METHOD

To understand along track image sharpness in a push broom imaging system, we model the nadir looking along track ge-

ometry (See Figure 1) using the physical parameters in Table 1. We call $T_f = \frac{1}{f_r}$ the frame period. The exposure time e may be set to any value in the range (T_{min}, T_f), independently from frame rate, where T_{min} is the minimum possible exposure time value, which may be much less than T_f or zero. A pinhole camera model is assumed and f and w determine the instantaneous along track field of view α. All parameters are assumed constant during an image acquisition, and the scene is assumed to be flat.

Table 1: List of parameters considered in this paper to model a Nadir looking push broom imaging system.

Parameter Name	Symbol	Note
Platform speed	v	
Platform height	h	
Focal length	f	
Slit width	w	
Frame rate & Frame period	f_r	$T_f = 1/f_r$
Exposure time	e	$e \in [T_{min},\, T_f]$

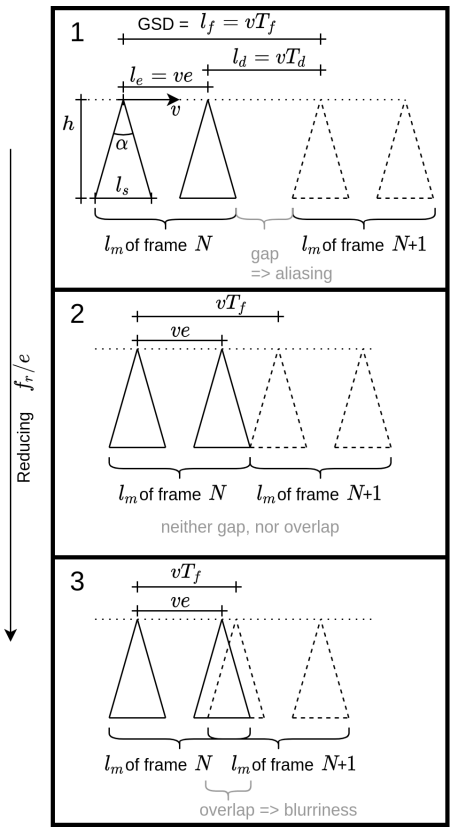

Fig. 1: Along track push-broom scanning geometry. The solid triangles represent the instantaneous along track field of view of the camera at the start and at the end of the exposure of a frame. The dashed triangles represent the same for the following frame.

With nadir pointing, the GSD is the distance the platform moves in a frame $l_f = v/f_r = vT_f$. Due to non zero along track field of view, the ground footprint of a single frame or exposure l_m is the distance moved during the exposure l_e, plus the swath width along track l_s

$$l_m = l_e + l_s = ve + h\frac{w}{f} \tag{1}$$

The ground footprint may also be viewed as the area from which light is collected to form a single pixel column or row in an image acquisition. The distance that subsequent frames are overlapping, or the gap size between subsequent frames, is

$$l_o = l_m - l_f = ve + h\frac{w}{f} - \frac{v}{f_r} \tag{2}$$

Finally, the overlap factor, the ratio between the overlap distance and the frame ground footprint is

$$o = \frac{l_o}{l_m} = 1 - \frac{T_f}{e + \frac{hw}{vf}}. \tag{3}$$

Depending on how less the exposure time e is compared to the frame period T_f, the along track geometry of an acquisition may fall into one of three cases: 1) gaps between frames, 2) no gap and no overlap, or 3) overlap between frames. The three cases corresponding to the three sub-figures in Figure 1.

If along track field of view is neglected, then case 3 is impossible, and case 2 is only achieved if $e = T_f$. However, if along track field of view is not neglected and the frame rate f_r is chosen so high such that the GSD is less than the ground length of the along track field of view, $l_f < l_s$, then it is impossible to choose the exposure time low enough, to avoid overlap between frames.

Let the time between when a frame has stopped being exposed to when the next frame starts to be exposed be called the *dark time*, $T_d = T_f - e$. Similarly, Let the distance the platform is moving from between frames when the sensor is not exposing be called *dark distance*, $l_d = vT_d$. If e is set to $T_f - \frac{hw}{vf}$ in Equation 3, then the overlap fraction is always 0. Thus $\frac{hw}{vf}$ is is the dark time such that there is neither overlap nor gap $T_{d,\text{nogap}} = \bar{T}_d = \frac{hw}{vf}$. $\bar{T}_d$ is also the time in which the platform moves a distance equal to the swath width l_s.

For HYPSO-1 with nadir pointing, having ca. $h = 520$km, $v = 7.615$km/s, $f = 50$mm and $w = 50$µm, [2, 9], we find that $\bar{T}_d$ is around 0.068 s. Thus, after the end of a frame exposure, the sensor must wait for around 68 milliseconds until the start of the exposure of the next frame to achieve no overlap. The dark time is, counter-intuitively, independent from the frame rate and exposure time setting. If the frame rate is larger than ca. $1/\bar{T}_d = 1/0.068$ s = 14.7 Hz, then, no matter the exposure time setting, successive frames will always overlap.

Overlap o means that there are locations in the scanned scene of which the reflected light is detected by multiple frames, causing along track blurriness. If the overlap factor is larger than 0.5, then there is a point in the scene that is covered by three frames. If the overlap factor is more than 0.66, then there is a point in the scene covered by four frames.

In general, the maximum count of frames which a point in the scene is covered by, can be expressed as $\left\lceil \frac{1}{1-o} \right\rceil$.

Equation 3 can be used to determine parameters for consistent overlap, leading to consistent along track sharpness. E.g. by choosing the value 0 for o, we get no gap and no overlap. Given $o = 0$, formulas can be derived to determine frame rate from a desired exposure time or exposure time for a given frame rate. These are

$$e = \frac{1}{f_r} - \bar{T}_d \,, \quad f_r = \frac{1}{e + \bar{T}_d} \tag{4}$$

In case of HYPSO-1 for example, if a low exposure of e.g. 10ms is required for a high reflectance target, the corresponding frame rate for no gap and no overlap is 12.82Hz. Similarly, an exposure time of 40ms results in frame rate 9.26Hz.

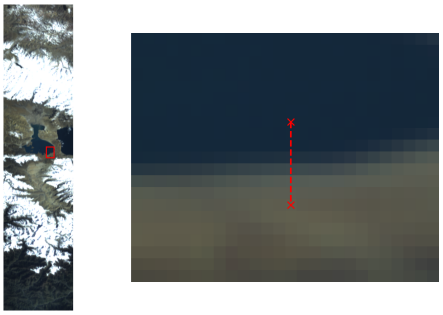

(a) Selected edge of an image acquisition. The edge response along the red dashed line is shown in the next subfigure.

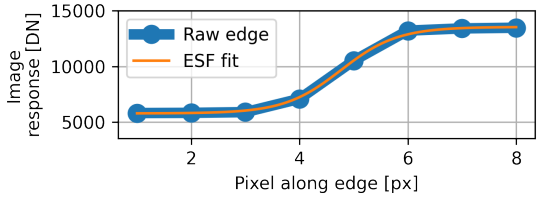

(b) Image edge response and the fitted ideal edge response.

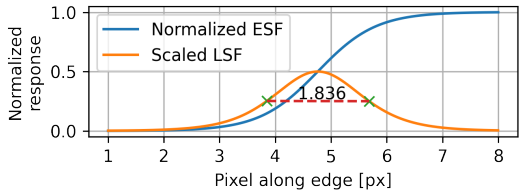

(c) Plot of the normalized edge response and the FWHM of the LSF.

Fig. 2: Figures illustrating the method to quantify sharpness of HYPSO-1 images.

To verify the method, the sharpness of acquired data must be quantified and compared to the predicted overlap based on the acquisition and platform parameters. The FWHM of the ESF is estimated using a simplified manual procedure compared to [8] as follows, see also Figure 2.

One of the sharpest edge of an image, found by visual inspection, is used for FWHM estimation. This is justified by noting that any variation of edge sharpness across an image is likely due to changes in the scene and not due to the optical system, as the optical system does not change across the short time of an acquisition. Following edge selection, the edge response is fit to a smooth ideal edge response function

$$f(x) = \frac{a}{1 + \exp\left(\frac{x-b}{c}\right)} + d \tag{5}$$

The fitted edge response function is then normalized into the range $[0, 1]$ and numerically differentiated to obtain the Line Spread Function (LSF). The FWHM of the LSF derived from the ESF is determined, and represents an estimate of the sharpness of the image. Only the sharpest band out of the 120 bands of the data from HYPSO-1 is considered for the FWHM estimation.

4. RESULTS

The HYPSO-1 satellite is not capable of recording hyperspectral data continuously. Data collection is grouped into small acquisitions with constant exposure time and frame rate. The results presented here are based on the analysis of 34 image acquisitions with different e and f_r with respect to predicted overlap and resulting FWHM of the ESF, see Figure 3. Out of the 34 acquisitions, nine had recording parameters chosen according to Equation 4 to achieve close to 0 overlap, see Figure 4 for their FWHM of the ESF.

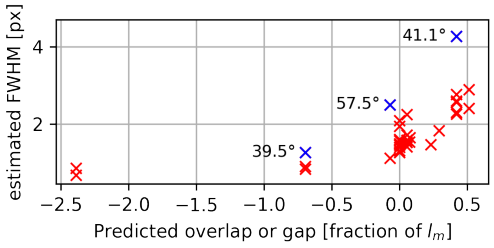

Fig. 3: Estimated FWHM of the ESF versus predicted overlap factor for 34 images from HYPSO-1. Each X represents one image. The three data points colored in blue are acquisitions at particularly large off-nadir angles, hence the large FWHM. The numbers in the figure indicate the off-nadir angle.

Figure 3 shows that there is a tendency for images to be less sharp with increasing positive overlap. Figure 3 further shows that image may be less sharp than predicted by overlap alone as indicated by the overlap and FWHM of the blue data points. These are image image acquisitions performed with large off-nadir angles, the off-nadir angle are indicated. Figure 4 plots the estimated FWHM of nine images, with f_r and e chosen for zero overlap, versus their off-nadir angle. This figure indicates consistent sharpness as desired. It also shows again a tendency for images to be more blurry with increasing off-nadir angle. Table 2 shows along track spatial

Table 2: The GRD illustrates diminishing returns when capturing data beyond a GSD of around 600m. The last capture illustrates the influence of large off-nadir angle on GRD.

GSD [m]	overlap	FWHM	GRD [m]	Off-Nadir
2362	-2.390	0.856	2021.5	23.59°
1180	-0.695	1.261	1488.3	39.52°
710	-0.071	1.114	791.0	0.42°
645	0.076	1.532	987.8	22.73°
443	0.292	1.836	813.3	13.30°
322	0.513	2.410	776.2	17.41°
710	-0.071	2.499	1773.9	57.52°

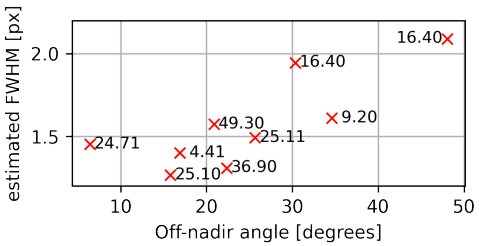

Fig. 4: Estimated FWHM of the ESF versus off-nadir angle for the nine acquisitions with capture parameters chosen for an overlap factor of zero. The numbers show the corresponding exposure times in [ms].

resolution figures of interest of an example set of six images sorted by decreasing GSD. While decreasing GSD does also decrease GRD, there are diminishing returns beyond a GSD of ca. 600m, a value close to the along track swath width of HYPSO-1 of 520m when nadir pointing. The seventh row in Table 2 shows how large off-nadir angle has a large effect on along track spatial resolution.

5. CONCLUSIONS

A relationship between overlap factor and FWHM of the ESF has been shown, verifying the simple geometric model and that along track field of view is an important aspect of a push broom imaging system to take into account. The overlap factor can be used to predict the sharpness of images from push broom imaging systems. The results clearly showed that the presented simple geometric model was not sufficient to explain all along track spatial resolution aspects, because it did not model off-nadir angles. Atmospheric scattering also may have contributed to varying sharpness of the images. However, the simple geometric model can provide a lower bound of image sharpness. Consistent sharpness over a exposure time range of 4.41 ms to 49.3 ms was achieved for low off-nadir angles. The manual method of estimating the FWHM of the ESF was not very reliable, so analyzing more data may increase accuracy.

Preliminary results were presented, giving a likely indication. Exhaustive analysis is subject to a possible future publication. A future publication might also consider how off nadir angle and slew maneuvers influence overlap and thus spatial resolution. Despite reduction of GSD beyond the point of zero gap did not increase along track spatial resolution, a large overlap could be exploited by super-resolution or deconvolution algorithms. These methods are already successfully used in snapshot images [10], and could also be successful in improving the spatial resolution of push broom images.

6. REFERENCES

[1] S. Bakken, M. B. Henriksen, et al., "Hypso-1 cubesat: First images and in-orbit characterization," *Remote Sensing*, vol. 15, no. 3, 2023.

[2] M. E. Grøtte, R. Birkeland, et al., "Ocean color hyperspectral remote sensing with high resolution and low latency–the hypso-1 cubesat mission," *IEEE Transactions on Geoscience and Remote Sensing*, pp. 1–19, 2021.

[3] M. Pepe, L. Fregonese, and M. Scaioni, "Planning airborne photogrammetry and remote-sensing missions with modern platforms and sensors," *European Journal of Remote Sensing*, vol. 51, no. 1, pp. 412–436, 2018.

[4] S. Ortega, R. Guerra, et al., "Hyperspectral push-broom microscope development and characterization," *IEEE Access*, vol. 7, pp. 122473–122491, 2019.

[5] A. U. G. Sankararao, S. K. N.T, D. Naresh, and P. Rajalakshmi, "Optimal parameter selection for uav based pushbroom hyperspectral imaging," in *2021 IEEE International India Geoscience and Remote Sensing Symposium (InGARSS)*, Dec 2021, pp. 413–416.

[6] Á. Q. Valenzuela and J. C. G. Reyes, "Basic spatial resolution metrics for satellite imagers," *IEEE Sensors Journal*, vol. 19, no. 13, pp. 4914–4922, 2019.

[7] Innovative Imaging and Research (I2R), "Spatial resolution digital imagery guideline," `https://www.usgs.gov/media/images/spatial-resolution-digital-imagery-guideline`, (Accessed on 2023-01-18).

[8] L. Cenci, V. Pampanoni, et al., "Presenting a semi-automatic, statistically-based approach to assess the sharpness level of optical images from natural targets via the edge method. case study: The landsat 8 oli–l1t data," *Remote Sensing*, vol. 13, no. 8, 2021.

[9] E. Prentice, M. E. Grøtte, F. Sigernes, and T. A. Johansen, "Design of hyperspectral imager using cots optics for small satellite applications," in *Int. Conf. Space Optics (ICSO)*, 2021.

[10] K. Nasrollahi and T. B. Moeslund, "Super-resolution: a comprehensive survey," *Machine Vision and Applications*, vol. 25, no. 6, pp. 1423–1468, aug 2014.